O- and N-glycosylation analysis of cell lines by ultrahigh resolution MALDI-FTICR-MS

Vreeker, G.C.M.; Nicolardi, S.; Madunic, K.; Kotsias, M.; Burgt, Y.E.M. van der; Wuhrer, M.

Citation
Vreeker, G. C. M., Nicolardi, S., Madunic, K., Kotsias, M., Burgt, Y. E. M. van der, & Wuhrer, M. (2020). O- and N-glycosylation analysis of cell lines by ultrahigh resolution MALDI-FTICR-MS. *International Journal Of Mass Spectrometry*, *448*. doi:10.1016/j.ijms.2019.116267

Version:	Publisher's Version
License:	Creative Commons CC BY 4.0 license
Downloaded from:	https://hdl.handle.net/1887/3181552

Note: To cite this publication please use the final published version (if applicable).

International Journal of Mass Spectrometry 448 (2020) 116267

Contents lists available at ScienceDirect

International Journal of Mass Spectrometry

journal homepage: www.elsevier.com/locate/ijms

O- and *N*-glycosylation analysis of cell lines by ultrahigh resolution MALDI-FTICR-MS

Gerda C.M. Vreeker [a, b], Simone Nicolardi [a, b], Katarina Madunic [a], Maximilianos Kotsias [a, c], Yuri E.M. van der Burgt [a], Manfred Wuhrer [a, *]

[a] Center for Proteomics and Metabolomics, Leiden University Medical Center, 2300 RC, Leiden, the Netherlands
[b] Department of Surgery, Leiden University Medical Center, 2300 RC, Leiden, the Netherlands
[c] Ludger Ltd, Culham Science Centre, Abingdon, Oxfordshire, United Kingdom

ARTICLE INFO

Article history:
Received 22 August 2019
Accepted 22 November 2019
Available online 26 November 2019

Keywords:
MALDI-FTICR-MS
High-resolution
Absorption mode
O-glycan
N-glycan

ABSTRACT

Glycosylation analysis from biological samples is often challenging due to the high complexity of the glycan structures found in these samples. In the present study *N*- and *O*- glycans from human colorectal cancer cell lines and human plasma were analyzed using ultrahigh resolution MALDI-FTICR-MS. *N*-glycans were enzymatically released from cell lines and plasma proteins, whereas beta-elimination was used for the release of *O*-glycans from the cells. The purified samples were mass analyzed using a 15T MALDI-FTICR-MS system, with additional MS/MS (collision-induced dissociation) experiments for *O*-glycan identifications. A total of 104 *O*-glycan and 62 *N*-glycan compositions were observed in the spectra obtained from colorectal cancer cell line samples. In the cell line *N*-glycan spectra, the highest intensity signals originated from high-mannose glycans, next to the presence of various complex type glycans. Notably, in the *O*-glycan spectra mono- and disaccharide signals were observed, which are difficult to detect using alternative glycomic platforms such as porous graphitized carbon LC-MS. In the *N*-glycan spectra from plasma, isobaric species were resolved in MALDI-FTICR-MS spectra using absorption mode whereas these overlapped in magnitude mode. The use of ultrahigh resolution MALDI-FTICR-MS for the analysis of glycans in complex mixtures enables us to confidently analyze glycans in the matrix region of the spectrum and to differentiate isobaric glycan species.

© 2019 The Authors. Published by Elsevier B.V. This is an open access article under the CC BY license (http://creativecommons.org/licenses/by/4.0/).

1. Introduction

Protein glycosylation is a common co- and post-translational modification that changes protein structure and function, and as a consequence plays an important role in various biological processes [1–4]. With regard to clinical utility and anticipated diagnostic applications, protein glycosylation changes have been studied for many different health conditions, aging, multiple types of cancer and autoimmune diseases [5–9]. The two main types of protein glycosylation are *N*- and mucin-type *O*-glycosylation.

Most *N*-glycans share a pentasaccharide core-structure and are attached to a specific asparagine in the protein backbone (consensus sequence Asn-X-Ser/Thr with X any amino acid except proline). *N*-glycans are often large, complex structures that have been studied extensively relying on their enzymatic release from protein backbones [10]. To study protein *N*-glycosylation various analytical methods are commonly used, including fluorescent labeling and detection, capillary electrophoresis, liquid chromatography (LC) and mass spectrometry (MS) [6,11–21].

Mucin-type *O*-glycans often vary vastly in size, from GalNAc monosaccharides attached to serine or threonine residues (Tn-antigens) to large oligosaccharides exhibiting a vast range of terminal glycan motifs. Notably, for a comprehensive analysis of *O*-glycans, a broad specificity release enzyme is lacking [18,22] and the analysis of *O*-glycans often relies on their chemical release from the protein backbone by reductive beta-elimination, resulting in glycan alditols that lack the reducing end for labeling with e.g. a fluorescent tag [23]. This makes MS-analysis the preferred method to characterize *O*-glycans, for example in combination with porous graphitized carbon(PGC)-LC-MS or as permethylated glycans using matrix-assisted laser desorption/ionization

* Corresponding author. Center for Proteomics and Metabolomics, Leiden University Medical Center, P.O. Box 9600, 2300 RC, Leiden, the Netherlands.
E-mail address: m.wuhrer@lumc.nl (M. Wuhrer).

https://doi.org/10.1016/j.ijms.2019.116267
1387-3806/© 2019 The Authors. Published by Elsevier B.V. This is an open access article under the CC BY license (http://creativecommons.org/licenses/by/4.0/).

Abbreviations

ACN	Acetonitrile
CEX	Cation-Exchange
CID	Collision Induced Dissociation
DTT	Dithiothreitol
EtOH	Ethanol
FTICR	Fourier-Transform Ion Cyclotron Resonance
LC	Liquid Chromatography
LLE	Liquid-Liquid Extraction
MALDI	Matrix-Assisted Laser Desorption/Ionization
MeOH	Methanol
MS	Mass Spectrometry
MQ	Milli-Q water
PGC	Porous Graphitized Carbon
TFA	Trifluoroacetic Acid
TOF	Time-Of-Flight

(MALDI)-MS [20,24]. It is noted that in both the PGC LC-MS workflows and in MALDI-MS the detection of short-chain *O*-glycans (mono- and disaccharide units) is prohibited because of loss during sample preparation and the overlap with matrix peaks, respectively. Of note, these small glycans are functionally relevant in cancer [25,26], and consequently methods are needed that allow the facile detection and characterization of these *O*-glycans from biological samples.

For glycan characterizations MALDI-MS is commonly performed on a time-of-flight (TOF) mass analyzer. However, the limited resolving power hampers identification of isobaric species in MALDI-TOF spectra [27]. In the case of *N*-glycans peak overlapping has been observed for large tri- and tetraantennary glycans [27] while for *O*-glycans high resolving power (RP) is needed to distinguish small structures from MALDI matrix signals. The highest RP and mass accuracy is obtained with Fourier transform ion cyclotron resonance mass spectrometer (FTICR-MS) [28]. The benefits of ultrahigh RPs have been demonstrated for the analysis of complex mixtures [29,30]. However, such high RPs generally come at the price of decreased sensitivities and longer measurement times [27]. Therefore, increasing RP post-acquisition by means of data processing is an attractive strategy.

The objective of the present study is to apply ultrahigh resolution MALDI-FTICR-MS for detailed *N*- and *O*-glycosylation analysis of complex samples. As an example, two cancer cell lines are selected, from which *N*-glycosylation MALDI-TOF profiles were previously reported by our group. In the current study the high RP of MALDI-FTICR-MS obtained in absorption-mode provides glycan profiles with low ppm mass precision that facilitates spectral alignment of multiple measurements or different samples. High RP of MALDI-FTICR-MS obtained in absorption mode allows the resolution of isobaric glycan species and provides glycan profiles with low mass measurement errors that facilitates spectral alignment of multiple measurements or different samples [31]. Furthermore, high mass accuracy over a large *m/z*-range improves *N*-glycan identifications. In addition, this study focuses on small *O*-glycans (mono- and disaccharides) in the matrix region of the MALDI-FTICR-MS spectra, to provide a complimentary strategy to porous graphitized carbon-LC-MS analysis.

2. Materials and methods

2.1. Materials

Plasma standard (Visucon-F frozen normal control plasma, pooled from 20 human donors, citrated and buffered with 0.02 M HEPES) was obtained from Affinity Biologicals (Ancaster, ON, Canada). Cancer cell lines SW48 and SW1116 were obtained from the Department of Surgery at Leiden University Medical Center (Leiden, The Netherlands). The 1.5 mL Eppendorf® Safe-Lock microcentrifuge tubes (Eppendorf tubes), potassium hydroxide (KOH), potassium borohydride (KBH4), glacial acetic acid, methanol (MeOH), mucin from bovine submaxillary glands (BSM) type I–S and Iodomethane (ICH3) were obtained from Sigma (Dorset, UK). The 96-well release plates (4ti-0125), the PCR plates, the foil pierce seals, the semi-automatic heat sealer (HT121TS), the polypropylene collection plates and the silicone plate lids were purchased from 4titude (Surrey, UK). The LudgerTagTM permethylation microplate kit (LT-PERMET-VP96) was obtained from Ludger Ltd (Oxfordshire, UK). The VersaPlate tubes were purchased from Agilent Technologies (Stockport, UK). The CEX resin (BIO-RAD, AG® 50W-X2 Resin) was purchased from Charlton Scientific (Oxon, UK). Trifluoroacetic acid (TFA), fetuin from fetal calf serum, tris(hydroxymethyl)aminomethane, sodium borohydride (NaBH4), Hydrochloric acid (HCl), DL-Dithiothreitol (DTT), 8 M guanidine hydrochloride (GuHCl), ammonium bicarbonate, 50% sodium hydroxide (NaOH), 1-hydroxybenzotriazole 97% (HOBt), super-DHB (9:1 mixture of 2,5-dihydroxybenzoic acid and 2-hydroxy-5-methoxybenzoic acid, sDHB), cation exchange resin Dowex 50W X8; cat. no. 217514 and ammonium acetate were obtained from Sigma Aldrich (Steinheim, Germany) and analytical grade ethanol, sodium chloride (NaCl) and methanol were purchased from Merck (Darmstadt, Germany). 1-Ethyl-3-(3-(dimethylamino)-propyl)carbodiimide (EDC) hydrochloride was purchased at Fluorochem (Hadfield, UK) and HPLC-grade acetonitrile (ACN) was obtained from Biosolve (Valkenswaard, The Netherlands). Ethylenediaminetetraacetic acid solution pH 8.0 and potassium hydroxide (KOH) were obtained from Fluka and PNGase F (Flavobacterium meningosepticum recombinant in *E. coli*; cat. no. 11365193001) and complete EDTA free protease inhibitor cocktail tablets were purchased at Roche. MultiScreen® HTS 96-multiwell plates (pore size 0.45 m) with high protein-binding membrane (hydrophobic Immobilon-P PVDF membrane) were purchased from Millipore, 96-well PP filter plate, cat.no. OF1100 from Orochem technologies (Naperville, USA), α2,3 neuraminidase, cat. no. GK80040) from New England Biolabs (Ipswich, MA, USA), SPE bulk sorbent Carbograph from Grace discovery sciences (Columbia, USA), Hepes-buffered RPMI 1640 culture media was purchased from Gibco (Paisley, UK). 0.5% trypsin-EDTA solution 10x was obtained from Santa Cruz Biotechnology (Dallas, USA), fetal bovine serum (FBS) and penicillin/streptomycin at Invitrogen (Carlsbad, USA). T75 cell culture flasks were purchased at Greiner-Bio One B.V. (Alphen aan de Rijn, The Netherlands). Milli-Q water (MQ) was generated from a QGard 2 system (Millipore, Amsterdam, The Netherlands), which was maintained at ≥18 MΩ. All automated steps in the analytical workflow described were performed using a Hamilton MICROLAB STARlet Liquid Handling Workstation from Hamilton Robotics Inc. (Bonaduz, Switzerland).

2.2. Cell culture

The cells were cultured as described in Holst et al. [32]. Pellets from three technical replicates of each cancer cell (~2 × 1000000 cells/technical replicate) were transferred into 1.5 mL Eppendorf tubes, and stored at −20 °C.

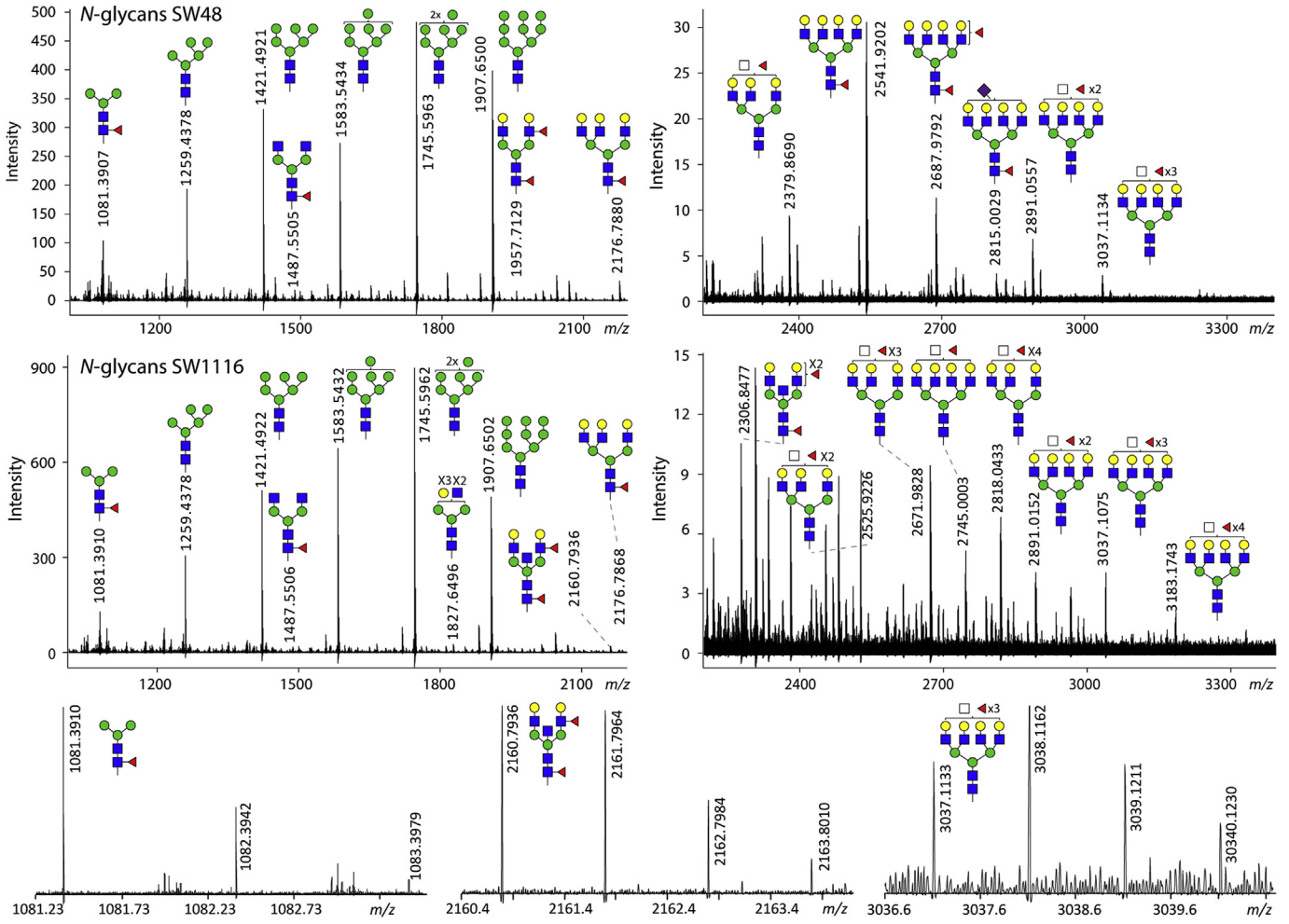

Fig. 1. Absorption mode MALDI-FTICR mass spectra of released and reduced *N*-glycans from cell lines SW48 and SW1116. All glycans are assigned as $[M+Na]^+$. Only the relevant *m/z*-range for glycans is shown.

2.3. *O*-glycan release and purification from cell lines

Cell pellets containing ca. 2 million cells were resuspended by pipetting action in 100 μL of water with resistivity 18.2 MΩ and homogenized for 90 min in a sonication bath. Following the disruption of cellular plasma membranes, each sample was manually transferred into a reaction well on the 96-well release plate. *O*-glycans were chemically cleaved from cell line proteins by semi-automated reductive β-elimination [33]. Briefly, the 96-well release plate containing the samples in-solution was placed on the robot deck. 40 μL of a 1 M KBH4 solution in 0.1 M KOH in water was dispensed into each reaction well and the contents were mixed by pipetting action. The release plate was sealed with a foil pierce seal in a semi-automatic heat sealer and incubated in an ultrasonic bath at 60 °C for 4 h off the robot deck. Following the incubation step, the release plate was briefly centrifuged in order to avoid cross contamination of samples. The seal was removed and the release plate was placed back on the robot deck where two aliquots of respectively 2 μL and 30 μL of glacial acetic acid were added to each reaction well to terminate the reductive β-elimination reaction.

Released *O*-glycans were purified by automated cation-exchange (CEX) cleanup, collected in a polypropylene collection plate and dried down in a centrifugal evaporator [33]. Following the automated cation-exchange cleanup, the polypropylene collection plate containing the dried samples was placed back onto the robot deck. A 1 mL aliquot of MeOH was dispensed into each well and the contents were mixed by pipetting action. Samples were dried down in a centrifugal evaporator.

2.4. Automated HT permethylation, liquid-liquid extraction (LLE) and MALDI-spotting

The released and purified *O*-glycans were permethylated using the LudgerTag™ permethylation microplate kit (LT-PERMET-VP96), purified by liquid-liquid extraction, dried down in a centrifugal evaporator and transferred to a PCR plate as previously described [18]. Permethylation and sample purification by liquid-liquid extraction were performed twice on the Hamilton MICROLAB STARlet Liquid Handling Workstation in order to reduce the percentage of partial permethylation and to improve the efficiency of the automated HT permethylation [18]. Samples were again dried down in a centrifugal evaporator in order to be concentrated prior to MALDI-FTICR-MS analysis. The samples were re-suspended in 10 μL of 70% methanol. The sDHB matrix (1.0 μL of 5 mg/mL super DHB with 1 mM NaOH in 50% ACN) was spotted on a MTP AnchorChip 800/384 MALDI-target (Bruker Daltonics) plate followed by 0.5 μL of permethylated sample and allowed to dry. Data acquisition was performed once for each sample on the MALDI-target plate using a 15T SolariX MALDI-FTICR-MS (Bruker Daltonics).

2.5. N-glycan release from cell lines

N-glycans were released from cell lysates of three technical replicates per cell line using a PVDF- membrane based approach as described previously [32]. Briefly, cell pellets were resuspended in lysis buffer (containing 50 mM Tris HCl, 100 mM NaCl, 1 mM EDTA, Protease inhibitor cocktail), sonicated for 1 h at 60 °C and proteins from ca. 500 000 cells were immobilized on a 96- well PVDF membrane filter plates in denaturing conditions by adding 72,5 μL of 8M GuHCl and 2,5 μL of 200 mM DTT and incubating for 1 h at 60 °C. After washing the samples with water to remove all the unbound material, *N*-glycans were released by adding 2 μL of PNGase F diluted in 13 μL of MQ to each well, incubating for 5 min, adding another 15 μL of MQ and incubating overnight at 37 °C. The glycans were recovered by centrifugation and washing (3 × 30 μL MQ) of the PVDF membrane. Subsequently 20 μL of ammonium acetate (pH 5) was added and incubated for 1 h. *N*-glycan reduction was performed as described before [20]. In short, 30 μL of 1 M NaBH4 in 50 mM KOH was added to the released glycans, incubated for 3 h, where after the reaction was quenched with 2 μL of glacial acetic acid. The glycans were desalted using strongly acidic cation exchange resin. 100 μL of resin in methanol was packed in the 96-well PP filter plate and three times washed with each of the following solutions: 100 μL of 1M HCl, 100 μL methanol and 100 μL water. The samples were loaded and elution was performed twice with 40 μL of MQ and centrifugation. Subsequently the samples were dried followed by borate removal with repeated methanol additions and drying (co-evaporation). Additional carbon solid phase extraction step was performed as described previously [20].

2.6. N-glycan derivatization, purification and MALDI-spotting

The dried samples were dissolved in 25 μL of MQ water. Then, 5 μL of this sample was added to 50 μL of ethylation reagent (0.25 M HOBt and 0.25 M EDC in EtOH) and incubated for one hour at 37 °C. After incubation 55 μL of ACN was added. Purification was performed as described before [27,34,35]. In short, in-house developed cotton-HILIC microtips were washed three times with 20 μL MQ and subsequently conditioned with three times 20 μL of 85% ACN. The sample was pipetted up-and-down twenty times in the cotton-HILIC tip and thereafter washed three times with 20 μL 85% ACN with 1% TFA and three times with 20 μL 85% ACN. To elute, 10 μL of MQ water was pipetted up-and-down five times. One microliter of sDHB-matrix (5 mg/mL with 1 mM NaOH in 50% ACN) was spotted onto a MALDI target plate (800/384 MTP AnchorChip, Bruker Daltonics, Bremen, Germany) with 5 μL of sample. The spots were left to dry and afterwards measured on a 15T SolariX MALDI-FTICR-MS instrument.

2.7. N-glycan analysis from plasma

Samples were prepared according to the previously published

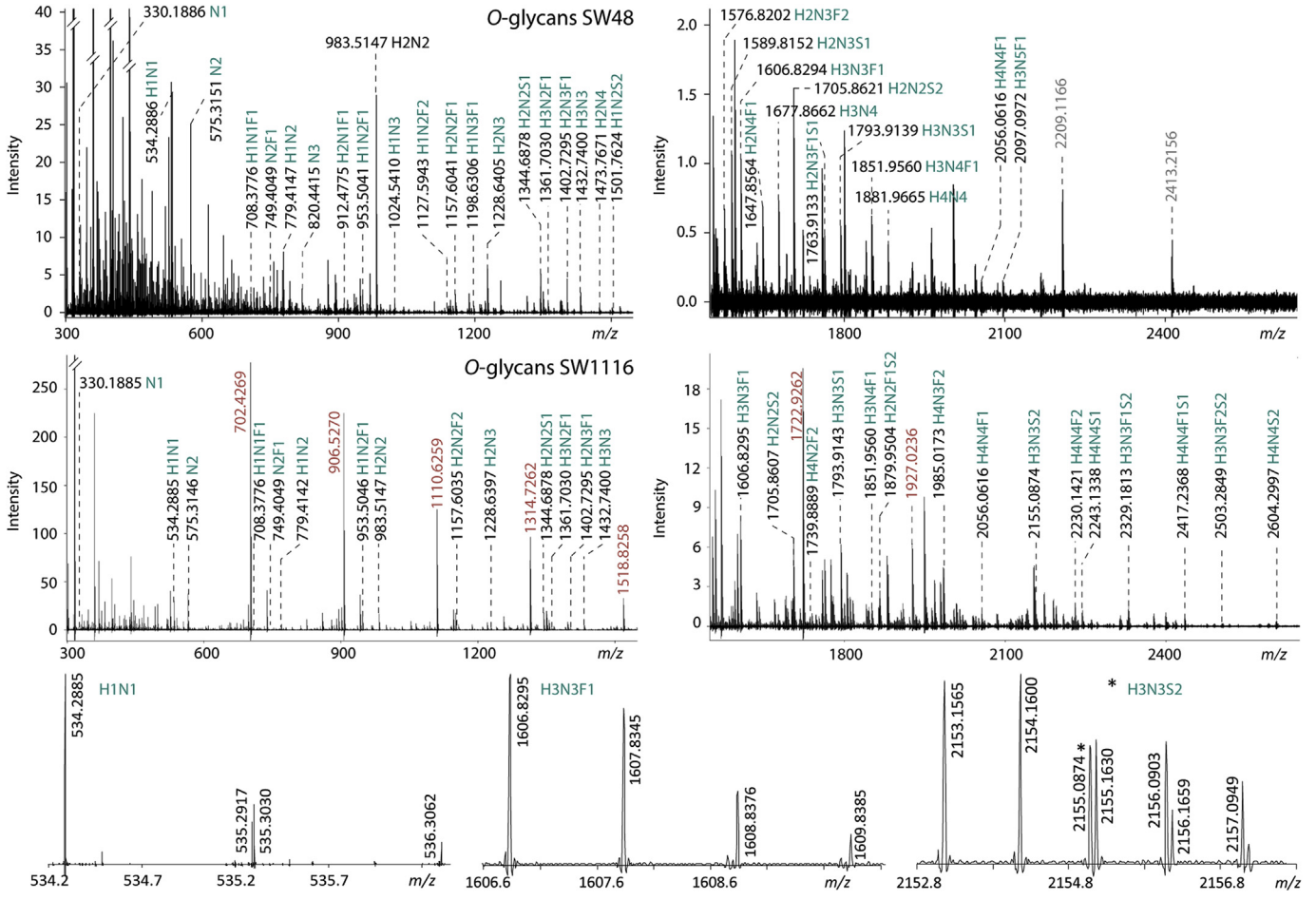

Fig. 2. Absorption mode MALDI-FTICR mass spectra of released, reduced and permethylated *O*-glycans from cell lines SW48 and SW1116. All glycan are assigned as $[M+Na]^+$, except for the hexose ladder (in red) in the *O*-glycan spectrum of SW1116, which carries a quaternary trimethyl ammonia group. Only the relevant *m/z*-range for glycans is shown. (For interpretation of the references to colour in this figure legend, the reader is referred to the web version of this article).

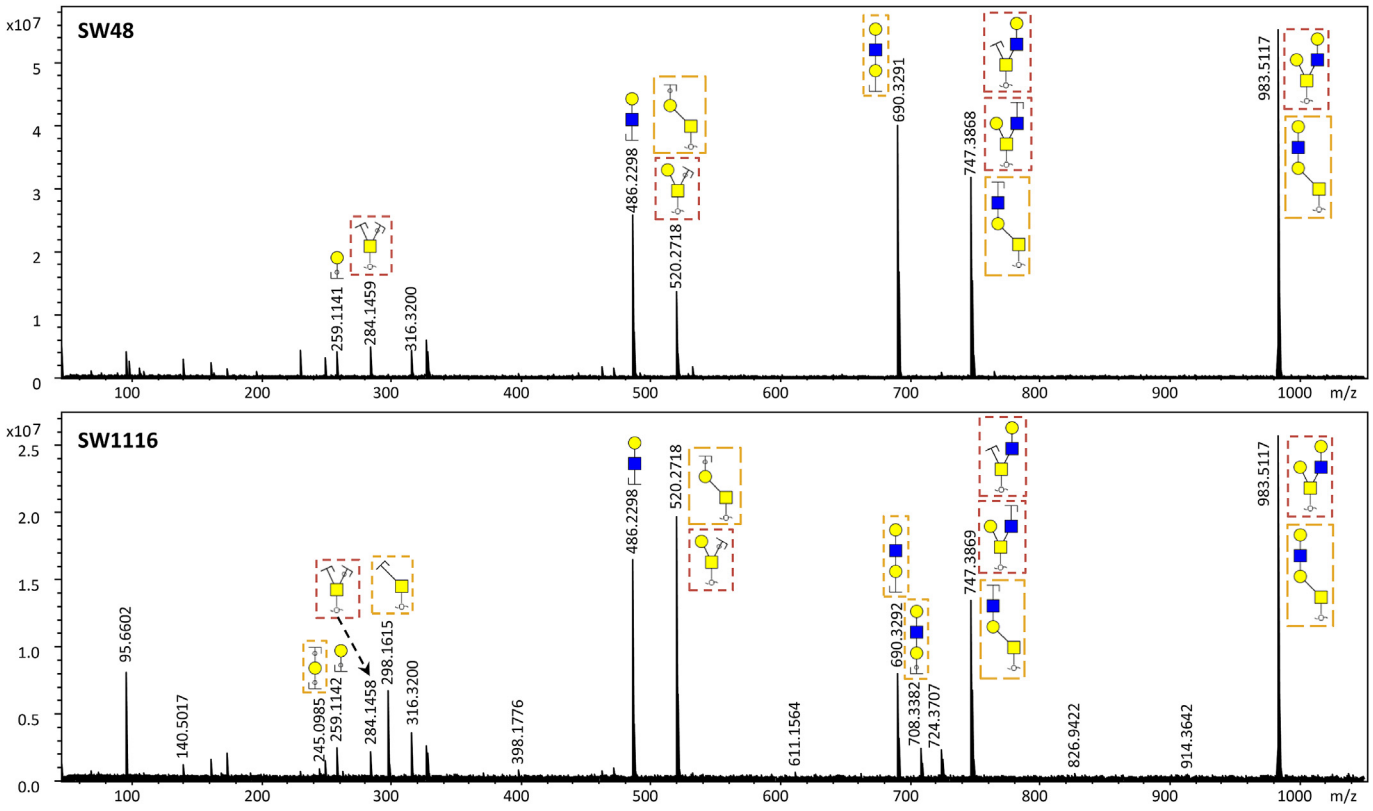

Fig. 3. Fragmentation spectrum of *m/z* 983.5117 which is assigned with the composition H2N2. The diagnostic ions (e.g. *m/z* 245, 284, 298, 690, 708) indicate that there are two different isomers of H2N2 present in the cell line samples.

method [27]. Briefly, the *N*-glycans were released from 6 μL Visucon plasma by first incubating the plasma for 10 min at 60 °C in 12 μL 2% SDS, where after the release mixture (6 μL acidified PBS, 6 μL 4% NP-40 and 0.6 μL PNGase F) was added and the sample was incubated overnight at 37 °C.

Automated derivatization, purification and MALDI-target plate spotting were performed using the liquid handling platform described before [27,36]. The carboxylic acid moieties of the sialic acids were derivatized by adding 2 μL of sample to 40 μL ethylation reagent (0.25 M EDC with 0.25 M HOBt in ethanol) and incubating for one hour at 37 °C. Subsequently 42 μL 100% ACN was added and after 10 min purification was performed in the same manner as described in 2.6, however, all amounts were doubled in the automated purification. MALDI-target spotting was performed as described in 2.6, but the sample and matrix volumes spotted were 2 μL and 1 μL respectively with premixing before spotting.

2.8. MALDI FT-ICR MS and MS/MS measurements

All MALDI-FTICR-MS measurements were performed on a 15T SolariX XR mass spectrometer (Bruker Daltonics) equipped with a CombiSource, a ParaCell and a SmartBeam-II laser system.

N-glycans were measured as previously reported. Briefly, for each MALDI spot, one spectrum consisted of ten acquired scans and 1 M data points was generated in the *m/z*-range 1011.86 to 5000.00. The laser was operated at a frequency of 500 Hz using the "medium" predefined shot pattern and 200 laser shots were collected per raster (i.e. 2000 per MALDI spot). The ParaCell parameters were as follows: both shimming and gated injection DC bias at 0°, 90°, 180°, and 270° were 9.20, 9.13, 9.20, 9.27 V, respectively; the trapping potentials were set at 9.50 and 9.45 V and the excitation power and sweep step time at 55% and 15 μs The transfer time of the ICR cell was 1.0 ms, and the quadrupole mass filter was set at *m/z* 850.

O-glycans spectra were generated from ten acquired scans and 1 M data points, in the *m/z*-range 207-5000. As for *N*-glycans, 200 laser shots were collected per raster using a 500 Hz laser frequency and the "medium" predefined shot pattern. The ParaCell parameters were as follows: both shimming and gated injection DC bias at 0°, 90°, 180°, and 270° were 1.20, 1.13, 1.20, 1.27 V, respectively; the trapping potentials were set at 1.50 and 1.45 V and the excitation power and sweep step time at 45% and 15 μs The transfer time of the ICR cell was 0.85 ms, and the quadrupole mass filter was set at *m/z* 100. Collision-induced dissociation (CID) experiments were performed with quadrupole (Q1) mass, isolation window and collision energy optimized for each precursor ion.

Absorption mode MALDI-FTICR-MS spectra were obtained using AutoVectis software (Spectroswiss, Lausanne, Switzerland) [37]. DataAnalysis Software 5.0 (Bruker Daltonics) and mMass [38] were used for the visualization and data analysis of MALDI-(CID)-FTICR-MS spectra.

3. Results and discussion

3.1. N- and O-glycan analysis with MALDI-FTICR-MS

Ultrahigh resolution MALDI-FTICR mass spectra were obtained from *N*- and *O*-glycans from two cell lines (referred to as SW48 and SW1116). In Fig. 1 annotated spectra of these cell lines for both glycosylation types are shown. The highest intensity signals found in the *N*-glycan spectra corresponded to high-mannose glycan structures. In addition, complex type glycans were annotated,

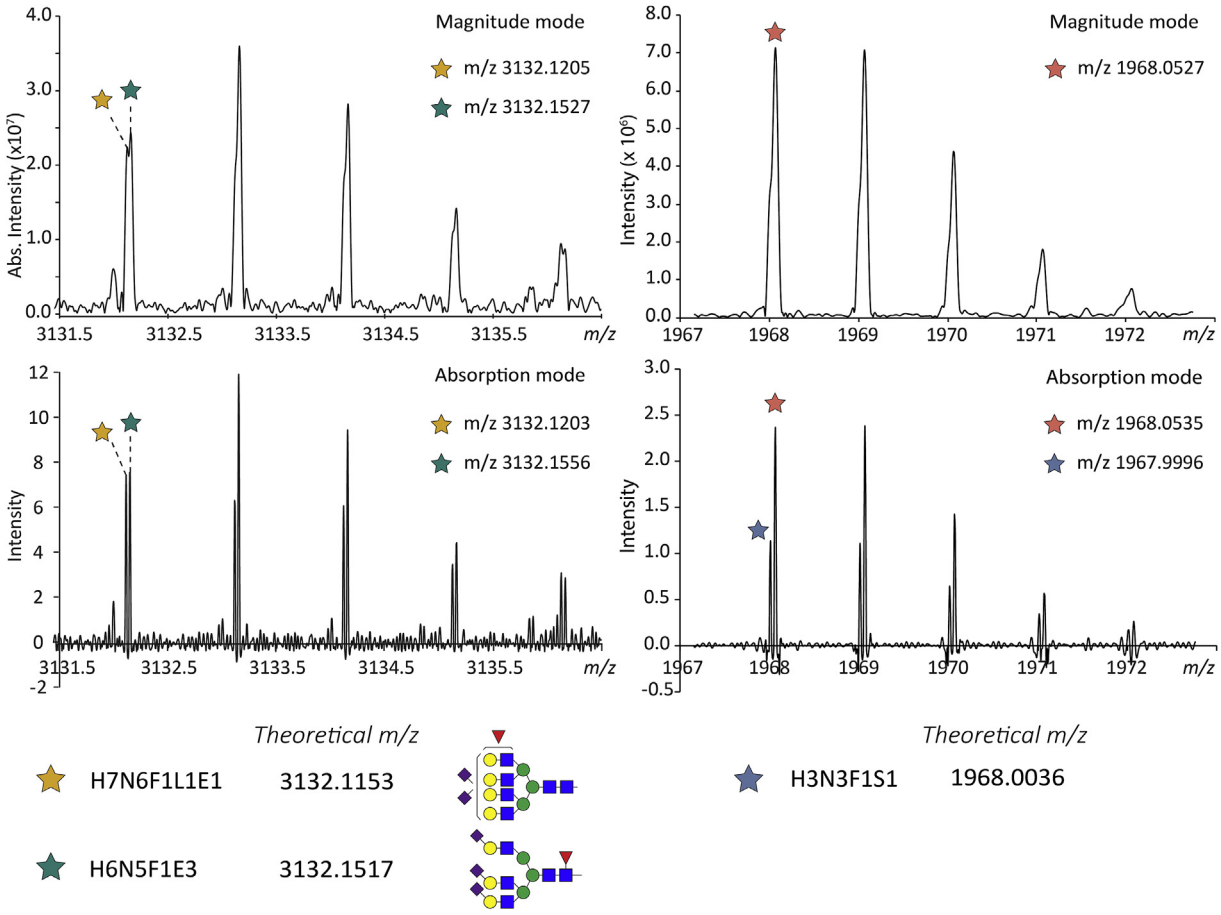

Fig. 4. Comparison of signals from MALDI-FTICR-MS measurements in magnitude mode and absorption mode. Due to increased resolution in absorption mode measurements the overlapping peaks are resolved. In de left panel two *N*-glycans are resolved and in the right panel an underlying *O*-glycan signal is resolved from an overlapping non-glycan analyte.

although observed at lower intensities. The total number of *N*-glycans detected in the spectra from SW48 and SW1116 were 76 and 104, respectively (see Tables S–1). Of all *N*-glycan assignments 94% were within a mass measurement error of ±2 ppm, with the remaining 6% within ±4 ppm, in a mass range of *m*/*z* 1000 to 3500. Remarkably, these high-accuracy assignments were reproducibly obtained from a single mass spectrum with lowest and highest glycan peak intensities varying by more than a factor of 5000.

In the *O*-glycan spectra of SW48 and SW1116 (Fig. 2), 44 and 62 *O*-different glycan compositions were annotated respectively (see Tables S–2). Of all *O*-glycan assignments 76% were within a mass measurement error of ±2 ppm and an additional 18% within ±6 ppm, in a mass range of *m*/*z* 300 to 3000. Similar to the spectra from the *N*-glycans the peak intensities varied by more than a factor of 5000. For many of these *O*-glycan compositions multiple glycan isomers are possible. This is exemplified in the fragmentation spectra of the sodiated permethylated alditol of the glycan composition H2N2 (Fig. 3). Diagnostic fragment ions are observed for both a linear and a branched tetrasaccharide structure (*m*/*z* 690.3291 and *m*/*z* 284.1459, respectively), and it is therefore concluded that this mass spectrometric signal represents a mixture of isomers. The linear glycan is proposed to be a core-1 *O*-glycan structure (Gal1-3/4GlcNAc1-3Gal1-3GalNAcitol) while the branched isomer is presumably a core-2 *O*-glycan structure (Gal1-3/4GlcNAc1-6[Gal1-3]GalNAcitol). In Figure S-1 additional fragmentation spectra are shown that demonstrate similar types of isomeric mixtures. Furthermore, high RPs in MALDI-FTICR spectra allowed detection of glycan signals in the matrix region. An interesting signal that was found corresponds to a single permethylated *N*-acetylhexosaminitol (*m*/*z* 330.19). This *N*-acetylhexosaminitol is most likely derived from a single GalNAc mucin-type *O*-glycan (Tn-antigen). Importantly, the Tn antigen cannot be detected with current PGC-LC-MS workflows for negative-mode analysis of native (*i.e.* non-permethylated) *O*-glycan alditols [20], and the mass spectrometric analysis of permethylated *O*-glycan alditols therefore represents a complementary technique making these biologically important short-chain *O*-glycans amenable for analysis. Next to the here presented MALDI-FTICR-MS analysis, the LC-MS analysis of permethylated glycans by reversed phase and porous graphitized carbon stationary phases has recently obtained increased attention. Such platforms may complement the MALDI-FTICR-MS approaches by providing isomer separation, as has recently been described for *N*-glycans [39–42].

Notably, it is still unclear to which extent other HexNAc sources such as protein-linked *N*-acetylglucosamine (*O*-GlcNAc) which is known to be mainly present on cytosolic proteins [43], may be contributing to the *N*-acetylhexosaminitol signal. MALDI-FTICR MS/MS analysis of permethylated *N*-acetylglucosaminitol and *N*-aceetylgalactosaminitol standards resulted in a similar fragmentation pattern for both species (data not shown), pointing out that additional experiments are needed in order to identify whether or not this signal is confounded by *O*-GlcNAc, and whether it can be largely attributed to the Tn-antigen.

Moreover, in Figure S-2 the full mass range of one *O*-glycan spectrum is shown, with a highly intense peak at *m*/*z* 316.32 that could be identified by MS/MS as dodecyl-bis(2-hydroxyethyl)-

methylazanium, a permanently charged compound originating from plastics. Further optimizations in the sample workup and purifications are therefore needed to turn these *O*-glycan spectra into robust profiles.

As a final remark on the *O*-glycan spectra, it was noted that the most intense peaks in SW1116 corresponded to a hexose ladder (see Fig. 2). These signals were also observed in SW48 at a lower intensity. The hexose ladder can be explained by the release of part of the *N*-glycans in the beta-elimination reaction, resulting in the appearance of additional high mannose glycans, as these *N*-glycans were identified amongst the most abundant species in this cell line. The ladder contains up to nine hexoses and a remainder mass that was identified as a hexosamine with a quaternary methylated amine group, thus carrying a positive charge (see fragmentation data in Figure S-3). An overview of the observed *m/z* values from the hexose ladder is shown in Tables S−3. An additional confirmation for the hypothesis that the hexose ladder resulted from the high-mannose glycans was provided by the observation of two additional hexose ladders in the *O*-glycan spectra: both ladders likewise consisted of up to nine hexoses with a *N*-acetylhexosamine or a hexosamine, which both ionized as [M+Na]+. The observed *m/z* values of these ladders are also shown in Tables S−3.

3.2. Resolving glycan signals

The measurements on *N*- and *O*-glycans from cell lines were compared with previous measurements performed in our group on released *N*-glycans from plasma [27]. Moreover, in the current study we evaluated the *N*-glycan MALDI-FTICR data from plasma in absorption mode instead of magnitude mode, resulting in a further improved resolution. Previously we reported that isobaric structures such as H7N6F1L1E1 and H6N5F1E3 were not distinguishable in MALDI-time-of-flight (TOF)-MS, and that overlapping signals were observed with magnitude mode measurements in MALDI-FTICR-MS [27]. Now, with absorption mode evaluation of the signals these two glycans are fully resolved (see Fig. 4). In the *O*-glycans spectra from cell lines this same effect is shown (Fig. 4 and S-4). The signal, assigned as H3N3F1S1, is in absorption mode separated from the overlapping signal in magnitude mode.

4. Conclusion

This study demonstrated that MALDI-FTICR-MS analysis allows for glycan identifications in complex mass spectra with low ppm mass measurement errors. However, a confident assignment of monosaccharide composition will not resolve the issue that complex biological samples often contain multiple glycan isomers. To this end diagnostic fragment ions in CID-spectra assist structure elucidation, as was exemplified in this study. In case overlapping signals were observed in MALDI-FTICR-MS absorption mode visualizations were a useful approach for increasing resolution and improving *O*- and *N*-glycan identifications. The benefits of ultrahigh RPs allow the analysis of complex samples, such as a *N*- or *O*-glycome, without the need for time consuming chromatography. The here presented strategy with low ppm mass measurement errors and confident glycan compositional assignment holds great potential for a comparative study on patient sample cohorts, such as plasma samples or cell lines.

Acknowledgements

The society “Genootschap ter ondersteuning van de vroege opsporing van kanker” (Lisse, The Netherlands) financially supported parts of this research performed at the LUMC to further endorse the development of a blood-based test for early detection of cancer (no grant number applicable). Katarina Madunic and Maximilianos Kotsias were supported by the European Commission Horizon 2020 programme under grant agreement number 676421 (GlyCoCan project).

Appendix A. Supplementary data

Supplementary data to this article can be found online at https://doi.org/10.1016/j.ijms.2019.116267.

References

[1] H. Geyer, R. Geyer, Strategies for analysis of glycoprotein glycosylation, Biochim. Biophys. Acta Protein Proteonomics 1764 (2006) 1853−1869, https://doi.org/10.1016/j.bbapap.2006.10.007.
[2] R.D. Cummings, The repertoire of glycan determinants in the human glycome, Mol. Biosyst. 5 (2009) 1087, https://doi.org/10.1039/b907931a.
[3] A. Dell, H.R. Morris, Glycoprotein structure determination by mass spectrometry, Science (80-) 291 (2001) 2351−2356, https://doi.org/10.1126/science.1058890.
[4] R.G. Spiro, Protein glycosylation: nature, distribution, enzymatic formation, and disease implications of glycopeptide bonds, Glycobiology 12 (2002) 43R−56R.
[5] A. Bondt, Y. Rombouts, M.H.J. Selman, P.J. Hensbergen, K.R. Reiding, J.M.W. Hazes, R.J.E.M. Dolhain, M. Wuhrer, IgG Fab glycosylation analysis using a new mass spectrometric high-throughput profiling method reveals pregnancy-associated changes, Mol. Cell. Proteom. 31 (2014) 1−30, https://doi.org/10.1074/mcp.M114.039537.
[6] K.R. Reiding, A. Bondt, R. Hennig, R.A. Gardner, R. O'Flaherty, I. Trbojević-Akmačić, A. Shubhakar, J. Hazes, U. Reichl, D.L. Fernandes, M. Pucic-Bakovic, E. Rapp, D.I.R. Spencer, R. Dolhain, P. Rudd, G. Lauc, M. Wuhrer, High-throughput serum N-glycomics: method comparison and application to study rheumatoid arthritis and pregnancy-associated changes, Mol. Cell. Proteom. (2018), https://doi.org/10.1074/mcp.RA117.000454.
[7] R. Saldova, M.R. Wormald, R.A. Dwek, P.M. Rudd, Glycosylation changes on serum glycoproteins in ovarian cancer may contribute to disease pathogenesis, Dis. Markers 25 (2008) 219−232, https://doi.org/10.1155/2008/601583.
[8] W.R. Alley, M. Madera, Y. Mechref, M.V. Novotny, Chip-based reversed-phase liquid chromatography-mass spectrometry of permethylated N-linked glycans: a potential methodology for cancer-biomarker discovery, Anal. Chem. 82 (2010) 5095−5106, https://doi.org/10.1021/ac100131e.
[9] L.R. Ruhaak, H.W. Uh, M. Beekman, C.H. Hokke, R.G.J. Westendorp, J. Houwing-Duistermaat, M. Wuhrer, A.M. Deelder, P.E. Slagboom, Plasma protein N-glycan profiles are associated with calendar age, familial longevity and health, J. Proteome Res. 10 (2011) 1667−1674, https://doi.org/10.1021/pr1009959.
[10] A.L. Tarentino, C.M. Gómez, T.H. Plummer, Deglycosylation of asparagine-linked glycans by peptide: N-glycosidase F, Biochemistry 24 (1985) 4665−4671, https://doi.org/10.4052/tigg.5.163.
[11] S. Zhou, Y. Hu, J.L. Desantos-Garcia, Y. Mechref, Quantitation of permethylated n-glycans through Multiple-Reaction Monitoring (MRM) LC-MS/MS, J. Am. Soc. Mass Spectrom. 26 (2015) 596−603, https://doi.org/10.1007/s13361-014-1054-1.
[12] S. Yang, D. Clark, Y. Liu, S. Li, H. Zhang, High-throughput analysis of N-glycans using AutoTip via glycoprotein immobilization, Sci. Rep. 7 (2017) 1−11, https://doi.org/10.1038/s41598-017-10487-8.
[13] C. Grünwald-Gruber, A. Thader, D. Maresch, T. Dalik, F. Altmann, Determination of true ratios of different N-glycan structures in electrospray ionization mass spectrometry, Anal. Bioanal. Chem. 409 (2017) 2519−2530, https://doi.org/10.1007/s00216-017-0235-8.
[14] Á. Szekrényes, S.A.S. Park, E. Cosgrave, A. Jones, T. Haxo, M. Kimzey, S. Pourkaveh, Z. Szabó, Z. Sosic, P. Feng, P. Sejwal, K. Dent, D. Michels, G. Freckleton, J. Qian, C. Lancaster, T. Duffy, M. Schwartz, J.K. Luo, J. van Dyck, P.K. Leung, M. Olajos, R. Kowle, K. Gao, W. Wang, J. Wegstein, S. Tep, A. Domokos, C. Váradi, A. Guttman, Multi-site N-glycan mapping study 2: UHPLC, Electrophoresis 39 (2018) 998−1005, https://doi.org/10.1002/elps.201700463.
[15] Y. Peng, J. Lv, L. Yang, D. Wang, Y. Zhang, H. Lu, A streamlined strategy for rapid and selective analysis of serum N-glycome, Anal. Chim. Acta 1050 (2019) 80−87, https://doi.org/10.1016/j.aca.2018.11.002.
[16] H.T. Le, K.H. Park, W. Jung, H.S. Park, T.W. Kim, Combination of microwave-assisted girard derivatization with ionic liquid matrix for sensitive MALDI-TOF MS analysis of human serum N-glycans, J. Anal. Methods Chem. 2018 (2018), https://doi.org/10.1155/2018/7832987.
[17] T. Keser, T. Pavić, G. Lauc, O. Gornik, Comparison of 2-aminobenzamide, procainamide and RapiFluor-MS as derivatizing agents for high-throughput HILIC-UPLC-FLR-MS N-glycan analysis, Front. Chem. 6 (2018) 1−12, https://doi.org/10.3389/fchem.2018.00324.
[18] A. Shubhakar, R.P. Kozak, K.R. Reiding, L. Royle, D.I.R. Spencer, D.L. Fernandes, M. Wuhrer, Automated high-throughput permethylation for glycosylation analysis of biologics using MALDI-TOF-MS, Anal. Chem. 88 (2016) 8562−8569, https://doi.org/10.1021/acs.analchem.6b01639.

[19] Y. Hu, T. Shihab, S. Zhou, K. Wooding, Y. Mechref, LC-MS/MS of permethylated N-glycans derived from model and human blood serum glycoproteins, Electrophoresis 37 (2016) 1498–1505, https://doi.org/10.1002/elps.201500560.
[20] P.H. Jensen, N.G. Karlsson, D. Kolarich, N.H. Packer, Structural analysis of N- and O-glycans released from glycoproteins, Nat. Protoc. 7 (2012) 1299–1310, https://doi.org/10.1038/nprot.2012.063.
[21] J.L. Abrahams, M.P. Campbell, N.H. Packer, Building a PGC-LC-MS N-glycan retention library and elution mapping resource, Glycoconj. J. 35 (2018) 15–29, https://doi.org/10.1007/s10719-017-9793-4.
[22] M.R. Kudelka, T. Ju, J. Heimburg-Molinaro, R.D. Cummings, Simple sugars to complex disease—mucin-type O-glycans in cancer, in: Adv. Cancer Res, 1st ed., Elsevier Inc., 2015, pp. 53–135, https://doi.org/10.1016/bs.acr.2014.11.002.
[23] G. Zauner, R.P. Kozak, R.A. Gardner, D.L. Fernandes, A.M. Deelder, M. Wuhrer, Protein O-glycosylation analysis, Biol. Chem. 393 (2012) 687–708, https://doi.org/10.1515/hsz-2012-0144.
[24] J.A. Goetz, M.V. Novotny, Y. Mechref, Enzymatic/chemical release of O-glycans allowing MS analysis at high sensitivity, Anal. Chem. 81 (2009) 9546–9552, https://doi.org/10.1021/ac901363h.
[25] Z. Liu, J. Liu, X. Dong, X. Hu, Y. Jiang, L. Li, T. Du, L. Yang, T. Wen, G. An, G. Feng, Tn antigen promotes human colorectal cancer metastasis via H-Ras mediated epithelial-mesenchymal transition activation, J. Cell Mol. Med. 23 (2019) 2083–2092, https://doi.org/10.1111/jcmm.14117.
[26] C. Fu, H. Zhao, Y. Wang, H. Cai, Y. Xiao, Y. Zeng, H. Chen, Tumor-associated antigens: Tn antigen, sTn antigen, and T antigen, Hla 88 (2016) 275–286, https://doi.org/10.1111/tan.12900.
[27] G.C.M. Vreeker, S. Nicolardi, M.R. Bladergroen, C.J. van der Plas, W.E. Mesker, R.A.E.M. Tollenaar, Y.E.M. van der Burgt, M. Wuhrer, Automated plasma glycomics with linkage-specific sialic acid esterification and ultrahigh resolution MS, Anal. Chem. 90 (2018) 11955–11961, https://doi.org/10.1021/acs.analchem.8b02391.
[28] D.P.A. Kilgour, R. Wills, Y. Qi, P.B. O'Connor, Autophaser: An algorithm for automated generation of absorption mode spectra for FT-ICR MS, Anal. Chem. 85 (2013) 3903–3911, https://doi.org/10.1021/ac303289c.
[29] S. Nicolardi, B. Bogdanov, A.M. Deelder, M. Palmblad, Y.E.M. Van Der Burgt, Developments in FTICR-MS and its potential for body fluid signatures, Int. J. Mol. Sci. 16 (2015) 27133–27144, https://doi.org/10.3390/ijms161126012.
[30] A.G. Marshall, R.P. Rodgers, Petroleomics: chemistry of the underworld, Proc. Natl. Acad. Sci. 105 (2008) 18090–18095, https://doi.org/10.1073/pnas.0805069105.
[31] S. Nicolardi, M. Palmblad, P.J. Hensbergen, R.A.E.M. Tollenaar, A.M. Deelder, Y.E.M. van der Burgt, Precision profiling and identification of human serum peptides using Fourier transform ion cyclotron resonance mass spectrometry, Rapid Commun. Mass Spectrom. 25 (2011) 3457–3463, https://doi.org/10.1002/rcm.5246.
[32] S. Holst, A.J.M. Deuss, G.W. van Pelt, S.J. van Vliet, J.J. Garcia-Vallejo, C.A.M. Koeleman, A.M. Deelder, W.E. Mesker, R.A. Tollenaar, Y. Rombouts, M. Wuhrer, N-glycosylation profiling of colorectal cancer cell lines reveals association of fucosylation with differentiation and caudal type homebox 1 (CDX1)/Villin mRNA expression, Mol. Cell. Proteom. 15 (2016) 124–140, https://doi.org/10.1074/mcp.M115.051235.
[33] M. Kotsias, R.P. Kozak, R.A. Gardner, M. Wuhrer, D.I.R. Spencer, Improved and semi-automated reductive β-elimination workflow for higher throughput protein O-glycosylation analysis, PLoS One 14 (2019) 1–14, https://doi.org/10.1371/journal.pone.0210759.
[34] M.H.J. Selman, M. Hemayatkar, A.M. Deelder, M. Wuhrer, Cotton HILIC SPE microtips for microscale purification and enrichment of glycans and glycopeptides, Anal. Chem. 83 (2011) 2492–2499, https://doi.org/10.1021/ac1027116.
[35] K.R. Reiding, D. Blank, D.M. Kuijper, A.M. Deelder, M. Wuhrer, High-throughput profiling of protein N-glycosylation by MALDI-TOF-MS employing linkage-specific sialic acid esterification, Anal. Chem. 86 (2014) 5784–5793, https://doi.org/10.1021/ac500335t.
[36] M.R. Bladergroen, K.R. Reiding, A.L. Hipgrave Ederveen, G.C.M. Vreeker, F. Clerc, S. Holst, A. Bondt, M. Wuhrer, Y.E.M. van der Burgt, Automation of high-throughput mass spectrometry-based plasma *N* -glycome analysis with linkage-specific sialic acid esterification, J. Proteome Res. 14 (2015) 4080–4086, https://doi.org/10.1021/acs.jproteome.5b00538.
[37] Y.E.M. van der Burgt, D.P.A. Kilgour, Y.O. Tsybin, K. Srzentić, L. Fornelli, A. Beck, M. Wuhrer, S. Nicolardi, Structural analysis of monoclonal antibodies by ultrahigh resolution MALDI in-source decay FT-ICR mass spectrometry, Anal. Chem. 91 (2019) 2079–2085, https://doi.org/10.1021/acs.analchem.8b04515.
[38] M. Strohalm, M. Hassman, B. Košata, M. Kodíček, mMass data miner: an open source alternative for mass spectrometric data analysis, Rapid Commun. Mass Spectrom. 22 (2008) 905–908, https://doi.org/10.1002/rcm.3444.
[39] S. Zhou, Y. Hu, Y. Mechref, High-temperature LC-MS/MS of permethylated glycans derived from glycoproteins, Electrophoresis 37 (2016) 1506–1513, https://doi.org/10.1002/elps.201500568.
[40] Y. Huang, S. Zhou, J. Zhu, D.M. Lubman, Y. Mechref, LC-MS/MS isomeric profiling of permethylated N-glycans derived from serum haptoglobin of hepatocellular carcinoma (HCC) and cirrhotic patients, Electrophoresis 38 (2017) 2160–2167, https://doi.org/10.1002/elps.201700025.
[41] S. Zhou, X. Dong, L. Veillon, Y. Huang, Y. Mechref, LC-MS/MS analysis of permethylated N-glycans facilitating isomeric characterization, Anal. Bioanal. Chem. 409 (2017) 453–466, https://doi.org/10.1007/s00216-016-9996-8.
[42] S. Zhou, K.M. Wooding, Y. Mechref, Analysis of permethylated glycan by Liquid Chromatography (LC) and mass spectrometry (MS), in: G. Lauc, M. Wuhrer (Eds.), High-Throughput Glycomics and Glycoproteomics, Springer New York, New York, NY, 2017, pp. 83–96, https://doi.org/10.1007/978-1-4939-6493-2.
[43] F.I. Comer, G.W. Hart, O -glycosylation of nuclear and cytosolic proteins, J. Biol. Chem. 275 (2002) 29179–29182, https://doi.org/10.1074/jbc.r000010200.